Modeling nitrogen deposition in global forests

Atmospheric Nitrogen Deposition to Global Forests

Schwede, Donna B.; Simpson, David; Dentener, Frank; Du, Enzai; de Vries, Wim

https://doi.org/10.1016/B978-0-323-91140-5.00009-9

Chapter 3

Modeling nitrogen deposition in global forests

Donna B. Schwede[a,1], David Simpson[b,c], Frank Dentener[d], Enzai Du[e,f] and Wim de Vries[g,h]

[a]*Office of Research and Development, United States Environmental Protection Agency, Durham, NC, United States;* [b]*EMEP MSC-W, Norwegian Meteorological Institute, Oslo, Norway;* [c]*Department of Space, Earth and Environment, Chalmers University of Technology, Gothenburg, Sweden;* [d]*European Commission, Joint Research Centre, Ispra, Italy;* [e]*State Key Laboratory of Earth Surface Processes and Resource Ecology, Faculty of Geographical Science, Beijing Normal University, Beijing, China;* [f]*School of Natural Resources, Faculty of Geographical Science, Beijing Normal University, Beijing, China;* [g]*Environmental Research, Wageningen University and Research, Wageningen, the Netherlands;* [h]*Environmental Systems Analysis Group, Wageningen University and Research, Wageningen, the Netherlands*

1. Introduction

Forests cover nearly one third of the land area and provide fundamental ecosystem services (Keenan et al., 2015). Nitrogen (N) availability limits plant growth and function in a considerable proportion of global forests, especially in high latitude and high elevation regions (Du et al., 2020). As an external nutrient input, atmospheric N deposition exerts profound effects on forest ecosystems (Du et al., 2019). These include a stimulation of forest growth and CO_2 sequestration in N-limited conditions (Gurmesa et al., 2022; Schulte-Uebbing and de Vries, 2018; Schulte-Uebbing et al., 2022). However, excessive N loads can cause a loss of species diversity (Bobbink et al., 2010; Gilliam et al., 2019; Simkin et al., 2016), an alteration of non-CO_2 greenhouse gases emissions (N_2O and CH_4) (Deng et al., 2020; Xia et al., 2020), soil acidification, an increase in the availability of toxic metals (Bowman et al., 2008), and imbalances between N and other nutrients (Du et al., 2016; Peñuelas et al., 2013). Considering the strong interactions with the canopy, the process of N deposition to the forest ecosystem is distinct from that measured in the open field (Du et al., 2014; Ignatova and Dambrine, 2000; Sparks, 2009). Therefore, understanding the spatial patterns and temporal dynamics of N deposition to global forests is a prerequisite to evaluate its ecological impacts and inform management strategies.

Several regional monitoring networks have been running to routinely measure atmospheric deposition of N and other elements (Dentener et al., 2006; Vet et al., 2014). Most of these monitoring networks are distributed in the northern hemisphere, such as the National Atmospheric Deposition Program in the United States, the European Monitoring and Evaluation Program, and the Acid Deposition Monitoring Network in East Asia (Beachley et al., 2023). Of these monitoring sites, many are located in or near forested environments and, together with independent and short-term studies, they have provided important insights into the characteristics of N deposition in regional forests (Du et al., 2014, 2016; Lovett and Lindberg, 1993; Waldner et al., 2014). However, monitoring data are lacking in many developing regions, especially in those of the southern hemisphere (Vet et al., 2014), hindering high-resolution and timely updated mapping of N deposition based on a spatial extrapolation of monitoring results. Global assessments and mapping of N deposition have thus been mostly dependent on atmospheric chemistry transport models that are regularly validated against field measurements (Dentener et al., 2006; Lamarque et al., 2013; Tan et al., 2018; Vet et al., 2014), but such assessments have rarely been conducted for regional and global forests (Schwede et al., 2018).

Nitrogen deposition has shown distinct long-term trends in its rates and components across different regions. For instance, N deposition has decreased in many developed countries in past decades (e.g., the United States, Europe and Japan) (Chiwa, 2021; Du et al., 2016; Waldner et al., 2014), while it has increased and will likely increase in many developing countries (Ackerman et al., 2019; Kulshrestha et al., 2014). In China, N deposition increased

1. Retired

Atmospheric Nitrogen Deposition to Global Forests. https://doi.org/10.1016/B978-0-323-91140-5.00009-9

dramatically from 1980 to 2010 (Liu et al., 2013) and thereafter has started to decrease mainly due to the efforts to curb NOx emissions (Wen et al., 2020). Moreover, atmospheric depositions of oxidized and reduced N species generally show different spatial patterns and temporal trends. For instance, Europe and the United States have been experiencing a decrease in atmospheric deposition of oxidized N, while the deposition of reduced N has remained high because NH_3 emissions have been less controlled (Du et al., 2016; Li et al., 2016; Schmitz et al., 2019; Waldner et al., 2014). These changes in rates and components of regional N deposition have important ecological implications in regional forests (Du et al., 2019). On a global scale, modeling efforts are needed to provide timely, updated maps of N deposition for the assessments of ecological impacts.

Plant growth and reproduction show specific phenological phases (e.g., leafing, flowering, fruit production and defoliation) that have different demands of nutrients and other resources (Fenner, 1998; Piao et al., 2019). Moreover, observational studies also show apparent seasonality of N deposition due to temporal variations in emissions, meteorology and surface parameters such as leaf area index (Liu et al., 2016; Zhao et al., 2015). This implies a temporally heterogeneous asymmetric effect of N deposition on forest ecosystems. Studies that neglect the seasonality of N deposition might result in uncertainties in assessing its ecological effects. For instance, N deposition in the growing season likely exerts a stronger stimulation of forest growth than N deposition during the nongrowing season in N-limited temperate and boreal forests. Therefore, assessing the seasonality of N deposition is relevant but such a global assessment is still lacking.

Based on a literature review, this chapter briefly summarizes the approaches in modeling N deposition (both wet and dry deposition) to forests and reviews the modeling studies of N deposition to regional and global forested areas. Furthermore, this chapter presents modeling estimates of N deposition (base year 2015) and its components (wet versus dry, oxidized N versus reduced N) across global forests using the Meteorological Synthesizing Center—West of the European Monitoring and Evaluation Program (EMEP MSC-W) model (Simpson et al., 2012, 2021). Particularly, modeling results are analyzed for forest-specific deposition and are calculated on an annual basis and for four 3-month periods (December−February, March−May, June−August, and September−November) to show the seasonality of N deposition in global forests.

2. Approaches and uncertainties in modeling deposition to forests

Estimates of atmospheric N deposition are an important input for ecological assessments and can be used to assess the effectiveness of a variety of policies that regulate the emissions of NO_x and NH_3, from large industrial scales to nutrient management plans on farms. Certainly, high-resolution and observationally based estimates of wet/dry deposition would ideally provide the most accurate estimates. Chapter 2 of this book provides a detailed description of monitoring efforts in forest systems including routine monitoring as well as special studies. Measurements of dry deposition continue to be a large gap in monitoring since it is more difficult and more expensive to measure than wet deposition and it is challenging to measure all components of the nitrogen budget (Walker et al., 2019). Notably absent from most measurements are values for the deposition of gaseous HNO_3, peroxyacyl nitrates (PANs), NO_2, and NH_3. There is a particular need for temporally-resolved and high-quality flux measurements of these compounds to promote process level understanding of air-surface exchange processes. Measurement data are also often missing for organic N which may comprise 20%−30% on average of the total reactive N in precipitation with variations from site to site (Du and Liu, 2014; Kanakidou et al., 2016; Neff et al., 2002). Additionally, there are large areas of the world where measurements are sparse. Modeling is a useful tool for providing spatially and temporally continuous values of wet and dry deposition. In this chapter, we review some of the conceptual frameworks for modeling N deposition. More detailed discussions can be found elsewhere (Fowler et al., 2009; Schwede et al., 2018; Wesely, 1989; Zhang et al., 2003) and a comprehensive review is beyond the scope of this chapter. The intent here is to provide an overview of approaches and uncertainties in modeling atmospheric N deposition to forests, examine spatial and temporal patterns of N deposition, and highlight opportunities and needs for further analyses.

2.1 Wet deposition

Wet deposition encompasses both in-cloud and below-cloud (rain/snow) scavenging and is typically modeled using chemical transport models (CTM) with modeled meteorology as input or coupled meteorological-chemical transport models. Approaches used to predict cloud cover amounts as well as precipitation rate, intensity, location, and type differ among meteorological models. This, in combination with the approaches for aqueous chemistry modeled in the CTM, can lead to very different estimates of wet deposition. Precipitation is notably difficult to predict using meteorological models which can lead to uncertainties in wet deposition values. Accuracy in modeled precipitation is also affected by model resolution, both vertically and horizontally as changes in surface characteristics will impact predicted model parameters. Many sensitive forest ecosystems occur in high elevation areas which are among the most challenging regions to model for clouds and precipitation. Additionally, fog deposition can

be significant in these high elevation areas and these local phenomena are difficult for models to predict and is only recently being included in some models (Katata, 2014).

For deposition of gaseous pollutants, another important consideration is the solubility of the pollutant. Most models use the Henry's Law constant to specify the solubility of a chemical species but may use different values. Sander (2015) provides a review of the range of Henry's Law constants for a large number of chemicals and illustrates the uncertainty associated with this parameter. The diffusion across the air/water interfacial surface is an important component and can be described using kinetic mass transfer and this process has recently been added to aqueous chemistry modules (Fahey et al., 2017). For aerosols, in-cloud scavenging depends on the effective activation of cloud droplets. Below-cloud scavenging of aerosols was reviewed by Zhang et al. (2013) and Wang et al. (2010) who noted that scavenging depends on raindrop and particle size and precipitations intensity. Wang et al. (2010) suggest that values of the scavenging coefficient could vary by as much as a factor of 5 due to uncertainties in the raindrop size distribution, collection efficiency and other factors which then translates into uncertainty in modeled values of deposition. Vet et al. (2014) provides an extensive review of global estimates of wet deposition, including modeled values obtained from global chemical transport models that participated in the Hemispheric Transport of Air Pollution (HTAP) project. This is an extremely useful data set; however, it should be recognized that the modeling for HTAP was performed at a coarse grid size of typically 2−3 degrees (regridded to a common 1×1 degree grid). Substantial spatial variability in precipitation can occur which may not be well captured by coarse grid sizes and should be considered in assessing modeled wet deposition to individual forested areas.

2.2 Dry deposition

Total dry N deposition is typically dominated by gaseous deposition of HNO_3 and NH_3 with smaller contributions coming from deposition of NO, NO_2, particulate NO_3^- (pNO_3), particulate NH_4^+ (pNH_4), and organic N (OrgN). Fig. 3.1 illustrates chemical species-specific deposition to three continents as calculated with the EMEP model for four seasons in 2015. For this analysis, we identified four 3-month periods: December, January, February (DJF; December 2015 was combined with January and February 2015); March, April, May (MAM); June, July, August (JJA), and September, October, November (SON). In all regions, HNO_3 and NH_3 are seen to be the largest contributors to N deposition, with a particularly large contribution of NH_3 in the MAM period. Both NO_2 and pNO_3 are the other large contributors from the NO_y species where NO_y includes all oxidized N species including NO, NO_2, HNO_3, N_2O_5, pNO_3, PANs (in EMEP: peroxyl acetyl nitrate (PAN) and methyl peroxyl acetyl nitrate (MPAN)), other organic nitrates (o-OrgN in Fig. 3.1), and other NO_y (o-NO_y in Fig. 3.1, comprised of HO_2NO_2 and HONO). In JJA, both the PANs and the o-OrgN are more significant than in DJF, reflecting both increased photochemistry and increased emissions of isoprene which contribute to isoprene nitrate in the o-OrgN compounds. Reduced N species also make large contributions to deposition in all seasons, though largest in MAM, with NH_3 being the dominant deposited compound. It should be noted that the dramatic peak in MAM for NH_3 stems from the assumed monthly variations used in the model. In these runs ECLIPSE data (International Institute for Applied Systems Analysis, 2021) are used, and a strong peak is seen in May for most of the Northern hemisphere. Results from model runs (not shown) using data from the CAMS-GLOB-ANT database (Granier et al., 2019) shows a much smaller spring peak. Guevara et al. (2021) also noted that different inventories have very different seasonal patterns for NH_3 emissions; these differences warrant further study as these seasonal patterns impact not only deposition estimates, but also our ability to evaluate model performance.

Several comparisons of approaches for modeling deposition of gases have been published including Flechard et al. (2011, 2013), and Wu et al. (2018). Gaseous dry deposition is typically modeled using a resistance framework, e.g.,

$$v_d = (R_a + R_b + R_c)^{-1} \tag{3.1}$$

where R_a is the aerodynamic resistance (s m^{-1}), R_b is the quasi-laminar boundary layer resistance (s m^{-1}), and R_c is the canopy resistance (s m^{-1}), with the canopy resistance being comprised of several component resistances including stomatal, mesophyll, cuticular, and soil resistance. The approaches for calculating the resistances vary among models and values for the resistances depend greatly on the surface to which the gas is depositing as well as the chemical properties of the gas itself. For example, deposition of NO_2 occurs mainly by stomatal uptake (Raivonen et al., 2009). There are many factors, both meteorological and biological that control stomatal uptake and the approach for modeling these factors varies across models resulting in different values across tree species or types (e.g., deciduous, coniferous). Other compounds such as HNO_3 deposit readily to surfaces with a deposition velocity that is typically controlled by the aerodynamic resistance. The aerodynamic resistance depends on the roughness of the surface as reflected in the surface roughness value, the canopy height, and the friction velocity. These values can vary across forests depending on many factors including tree species present, the height of the trees, and spacing of the trees. Chemical transport models often assign a single value for each forest type (e.g., deciduous, coniferous) and are unable to account for differences in species composition or forest

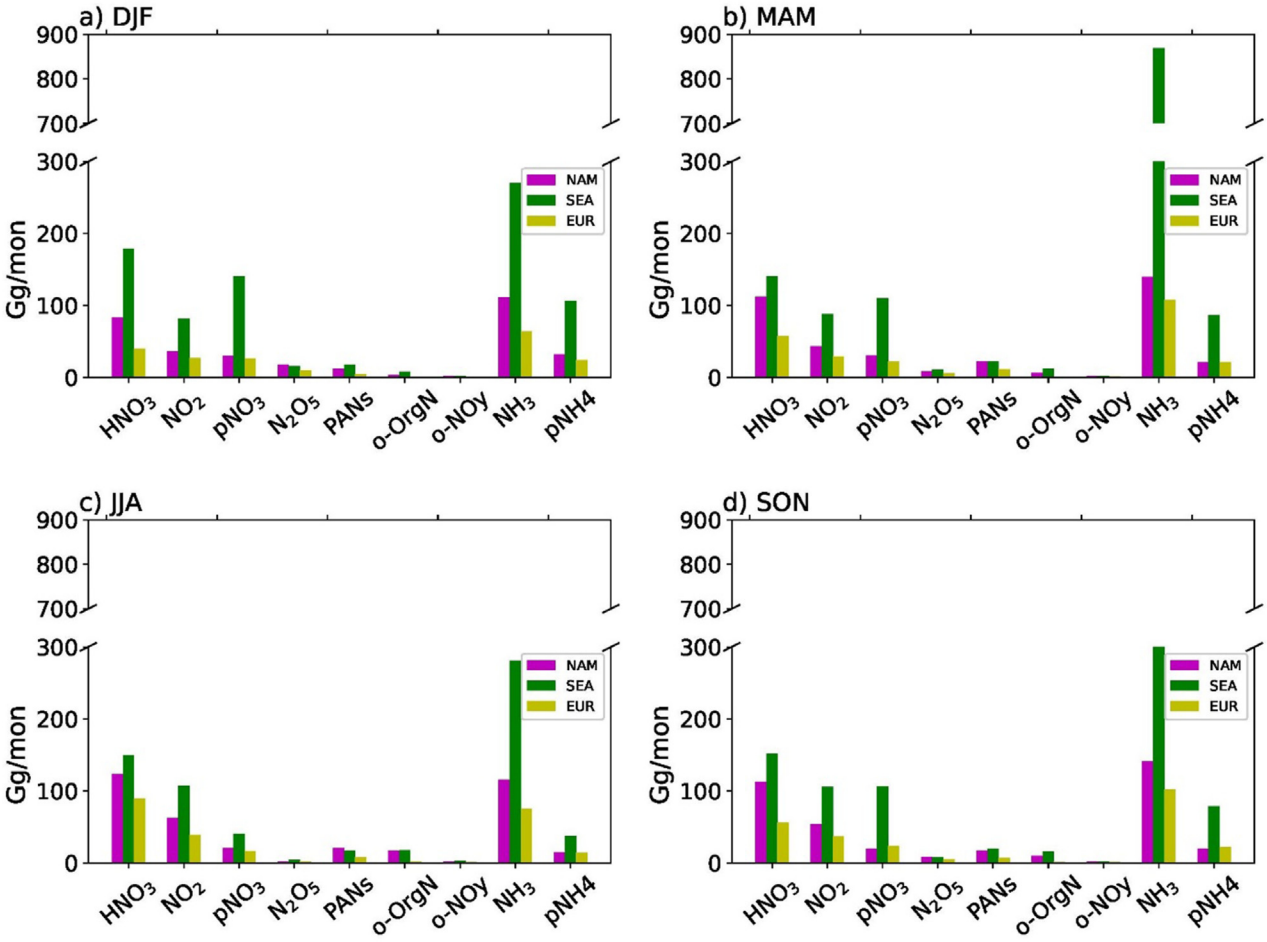

FIG. 3.1 Contributions of N-compounds to N deposition over regions denoted Europe (EUR, 37−75°N, 15°W−50°E), North America (NAM, 13−75°N, 40−170°W) and South East Asia (SEA, 10°S−37°N, 65−170°E) for four periods: (A) DJF (December, January, February), (B) MAM (March, April, May), (C) JJA (June, July, August), and (D) SON (September, October, November). See text for species definitions. Calculations from EMEP MSC-W model for 2015.

architecture. So, in some models the sequoia forests of California in North America and the larch trees of a northern boreal forest might both be modeled with similar values of important parameters such as leaf area index, canopy height, and roughness length. New data sets such as the Global Forest Canopy Height (https://glad.umd.edu/dataset/gedi) which provides maps of forest canopy heights at 30-m resolution will be an important resource for improving modeled characterizations of forests. Site-based models are typically driven by measured values or site-specific values that account for the tree species found at that location. Deposition velocities of HNO_3 for forests are generally around 2−4 cm s^{-1} (Pryor et al., 2002), though an important issue is that HNO_3 is only measured at a limited number of sites globally. This high deposition velocity is, in part, why deposition of HNO_3 is such a large component of the total N budget.

Air-surface exchange of NH_3 is a much more complex calculation as in principle one should account for the bidirectional nature of the flux. The flux parameterization for NH_3 can take the form of

$$F = \frac{-(\chi_a - \chi_{z_0})}{R_a} \tag{3.2}$$

as in Nemitz et al. (2001) and Massad et al. (2010) where X_a is the ambient ammonia concentration, X_{z0} is the concentration at a height of $d + z_0$ (also called compensation point) with d being the displacement height and z_0 being the roughness length. The direction of the flux will be downward (deposition) if X_a exceeds X_{z0} and will be upward (emission) if X_a is less than X_{z0}. While leaf litter in forests can be a source of ammonia (Hansen et al., 2013), overall NH_3 flux to the forest is generally downward (deposition).

Modeling dry deposition of particles to forests has been shown to be challenging (Emerson et al., 2020; Fowler et al., 2009; Pryor et al., 2008; Saylor et al., 2019). Most models follow the approach of Slinn (1982)

$$v_d = (R_a + R_s)^{-1} + v_g \quad (3.3)$$

where R_a is the aerodynamic resistance (s m^{-1}), R_s is the surface resistance (s m^{-1}), and v_g is the gravitational settling velocity (s m^{-1}). The surface resistance is parameterized to consider the collection efficiency of the aerosols due to various processes including Brownian diffusion, interception by the vegetation, inertial impaction, electrophoresis, and thermophoresis. Similar to gases, the deposition velocity of aerosols is sensitive to the meteorology and the surface characteristics but also the particle size. Petroff et al. (2008a) and Pryor et al. (2008) provide extensive reviews of modeling approaches currently used in many atmospheric models.

Models differ in the treatment of the collection efficiency, with some models including more processes (e.g., interception, thermophoresis) than others. The extent to which different resistances and collection efficiencies are important varies with the size of the aerosol. New approaches for calculating the dry deposition of aerosols have recently been proposed including those by Petroff et al. (2008b), Petroff and Zhang (2010), Kouznetsov and Sofiev (2012), Zhang and He (2014), Zhang and Shao (2014) and Emerson et al. (2020). Emerson et al. (2020) use advanced measurement techniques to provide new size-resolved particle flux measurements over a pine forest and a grassland. Similar to Petroff and Zhang (2010), Emerson et al. (2020) suggest a far more important role for interception, particularly in forests. Since the deposition velocity is size dependent, differences in deposition flux between CTMs will also depend on the characterization of the phase of the pollutant (depending on relative humidity) and the size of the particle as predicted by the variety of aerosol modules in global models. There is a great need for additional size resolved measurements of aerosol deposition in forests to promote process level understanding of exchange processes to inform development of models with less dependence on empirical fits to observations.

2.3 Overview of modeling approaches and related studies

As noted above, models have an important role in providing spatially and temporally resolved and continuous estimates of total N deposition to forests. The two most common deposition modeling approaches are inferential models and chemical transport models while measurement-model fusion is an emerging type of deposition modeling, all being discussed more detail below.

2.3.1 Inferential models

In the inferential approach, a measured concentration is multiplied by a modeled exchange velocity (Wesely and Hicks, 2000). Dry deposition is often estimated using an inferential approach. For example, the Clean Air Status and Trends Network (CASTNET; http://www.epa.gov/castnet/) has followed this approach for many years to provide flux estimates of O_3, SO_2, HNO_3, pNO_3 and pNH_4 and other species for over 90 locations in the US. The Canadian Air and Precipitation Monitoring Network (CAPMoN; https://www.canada.ca/en/environment-climate-change/services/air-pollution/monitoring-networks-data/canadian-air-precipitation.html) also uses inferential modeling to predict deposition at over 50 sites in Canada. Most CAPMoN sites monitor a set of species similar to CASTNET. Different inferential modeling approaches have been used for each of these networks with intercomparisons(Schwede et al., 2011; Wu et al., 2018) indicating differences in deposition velocities that can be traced primarily to differences in the cuticular resistance and aerodynamic resistance parameterizations. Differences in deposition velocity predicted by the deposition modeling approaches can vary as much as a factor of 2 for Borden Forest in Canada (Wu et al., 2018). Flechard et al. (2011) applied the inferential approach to a network of 55 sites throughout Europe for a 2-year period as part of the NitroEurope Integrated Project (Tang et al., 2021). Their modeling predicted fluxes of HNO_3, NO_2, HONO, NH_3, pNO_3 and pNH_4 using 4 different deposition models. The study found that dry deposition was generally largest over forests but exhibited strong spatial variations due to differences in atmospheric concentration. Fluxes were less than 2 kg N ha^{-1} $year^{-1}$ in remote areas of Scandinavia but exceeded 30 kg N ha^{-1} $year^{-1}$ over parts of Belgium and the Netherlands. Fu et al. (2019) used the inferential approach to predict deposition to a forest in the North China plain. Their approach used the deposition velocities for forested areas from Flechard et al. (2011) paired with concentration measurements of HNO_3, NO_2, NH_3, pNO_3, and pNH_4 and estimated the total dry deposition to be about 44 kg N ha^{-1} $year^{-1}$.

An extension of the inferential modeling approach has been used to obtain deposition values at the landscape scale. The Empirical Inferential Method (EIM) is described in Bytnerowicz et al. (2015). EIM combines atmospheric concentrations from passive samplers with species specific surface conductance obtained from branch rinsing and stomatal conductance based on species-specific values from literature. Using this method, Bytnerowicz et al. (2015) were able to develop spatially continuous fields of deposition and capture important spatial gradients in complex terrain that were not predicted well by chemical transport modeling. Sensitive tree species are often found in high elevation areas, making these spatial gradients particularly

important. In a similar study García-Gómez et al. (2018) used EIM to predict deposition to several holm oak forests across the Iberian Peninsula, utilizing the Deposition of Ozone for Stomatal Exchange (DO_3SE) model (Alonso et al., 2008; Emberson et al., 2000) to determine the stomatal conductance.

2.3.2 Chemical transport models

Chemical transport models (CTMs) are another important tool for modeling deposition to forests that can provide temporally and spatially continuous predictions of deposition and also include portions of the total nitrogen budget that are often not available from measurement studies or inferential modeling. Numerous studies have used CTMs to predict deposition across individual countries and globally (Ackerman et al., 2019; Wang et al., 2017). Similar to inferential models, deposition values predicted by CTMs vary between models, with differences resulting from heterogeneity in emissions, meteorology, and model parameterizations including those for deposition. Multi-model studies such as the second phase of the Task Force on Hemispheric Transport of Air Pollution (HTAP II (Tan et al., 2018)), EURODELTA (Vivanco et al., 2018), Model Inter-Comparison Study for Asia (MICS-ASIA (Itahashi et al., 2020)) and the Air Quality Modeling Evaluation International Initiative (AQMEII; https://aqmeii.jrc.ec.europa.eu/) have been very important in analyzing model to model differences in concentration and deposition. CTMs are typically run with grid sizes of 0.5 × 0.5 degrees and greater for global assessments while grid sizes for regional modeling are on the order of 0.1 degree. At this resolution, there can be large subgrid variability in deposition due to concentration gradients, changes in land cover, changes in elevation, etc. that may not be captured by the CTM. Paulot et al. (2018) and Schwede et al. (2018) showed the importance of considering land use specific deposition estimates rather than simply grid cell average values. Phase 4 of AQMEII (Galmarini et al., 2021) is specifically focused on deposition and will include land use specific deposition values for all grid-based models as well as point-intercomparisons where the deposition models from the CTMs are used with field study data. Both the grid modeling and the point-intercomparison will also provide additional diagnostic variables that will help elucidate important differences in the parameterizations of the pathways of deposition. While these land use specific estimates from CTMs provide important subgrid scale information that can be important to assessing endpoint such as critical loads exceedances, they do not provide information on subgrid spatial gradients—i.e., a deciduous forest in one section of the grid will have the same flux as a deciduous forest in another section of the grid despite potential underlying concentration gradients that may actually occur. The grid-scale values and the land use-specific values both rely on the grid-averaged concentration of the chemical species. Chemical transport models also only typically model broad categories of land use types such as deciduous or coniferous trees. Species specific or location specific differences in key parameters such as minimum stomatal resistance, canopy height and leaf area index may not be considered which is a source of error or uncertainty in the deposition values. These uncertainties can be important to consider when using the modeling results to assess potential impacts for a specific forest.

2.3.3 Measurement-model fusion

An emerging type of modeling for predicting deposition is measurement-model fusion. Observational data, including information from ground-based measurements and satellite data, can be merged with data from CTMs in several ways. Vet et al. (2014) combined measurements of wet deposition with modeled values of wet and dry deposition to create global maps of deposition. In another approach, chemical data assimilation is used to ingest the observational data into the CTM as it is running to "nudge" the model toward the observed value (Bocquet et al., 2015; Sandu and Chai, 2011). Yet another approach post-processes the fields from the CTM to bias correct the model fields (Andersson et al., 2018; Schwede et al., 2019; Schwede and Lear, 2014; Zhang et al., 2019). The MMF approach is a current focus of the WMO-MMF-GTAD project that proposes to use this approach to develop global values of sulfur, N and ozone deposition (Fu et al., 2022). The MMF approach reduces model error that may result from errors in emissions, meteorology, or processes and future MMF products may also consider producing land use-specific values which would be of great value for assessments of deposition on forests.

3. Calculation of global scale total nitrogen deposition

3.1 Modeling approach

We examined the spatial distribution of total N deposition at the global scale as well as the contributions of wet versus dry N deposition and oxidized versus reduced N deposition using the EMEP MSC-W CTM model (hereafter EMEP model) which is a three-dimensional Eulerian model whose main aim is to support governments in their efforts to design effective emissions control strategies in Europe. The model has been extensively evaluated (Marchetto et al., 2021; Simpson et al., 2006; Theobald et al., 2019) and has also been widely used for global analyses (Jonson et al., 2018; Schwede et al., 2018; Tan et al., 2018). In addition to its long history of use, we selected the EMEP model for use

in this analysis as forest-specific global deposition fields are available from the EMEP model while most other models do not provide this level of detail. The EMEP model's chemical mechanism, EmChem19a (Bergström et al., 2022; Simpson et al., 2020), includes the inorganic species NO, NO_2, HNO_3, HONO, HO_2NO_2, NO_3, N_2O_5, fine and coarse nitrate, as well as PAN-like species (PAN, MPAN), and three other organic N species (Bergström et al., 2022). The model uses meteorology from the European Center for Medium Range Weather Forecasting Integrated Forecasting System (ECMWF-IFS) model (http://www.ecmwf.int/research/ifsdocs/). For this analysis, version rv4.44 of EMEP (Simpson et al., 2012, 2021) was run at the global scale at 0.5 × 0.5 degrees resolution with the lowest model layer having a height of approximately 90 m. Anthropogenic emissions are from the ECLIPSEv6b inventory (Evaluating the CLimate and Air Quality ImPacts of Short-livEd Pollutant) inventory (International Institute for Applied Systems Analysis, 2021; Klimont et al., 2017), with monthly variations for these data provided by the ECLIPSE team for use with the EMEP code. Monthly soil-NO calculations are from v2.3 of the CAMS-GLOB-SOIL inventory (Simpson et al., 2023) (excluding fertilizer-manure induced emissions, which are part of the ECLIPSE data). Total emissions from all sources into the model domain are 56.6 Tg(N) for NO_y and 53.4 Tg(N) for NH_x.

Dry deposition flux for gases in the EMEP model is modeled using the resistance approach with a reference height of approximately 45 m (mid-level of lowest model layer), which is considered to be within the constant flux layer. The model includes parameterizations for the aerodynamic, quasi-laminar and surface resistances. Important to the consideration of N deposition, the surface resistance for HNO_3 is considered to be effectively zero, with a minimum value of 10 s m^{-1} imposed for numerical reasons. For NH_3, the surface resistance for croplands is set to a large number during the growing season to force the deposition to be zero as most croplands exhibit a net emission of NH_3. Therefore, the more explicit bidirectional flux approach used in other models (Bash et al., 2013; Cooter et al., 2010; Massad et al., 2010; Nemitz et al., 2001; Pleim et al., 2013) is not implemented in the current version of the EMEP model. Since most flux to forests is primarily downward, lack of a bidirectional flux approach does not have strong implications for this analysis. At the reference height, concentrations and meteorological variables are assumed to be representative of the grid cell rather than a specific underlying land surface. The EMEP model uses a mosaic approach to deposition, which pairs the grid cell values with subgrid calculations of land cover-specific u_*, stability parameters, and resistances, as described in Simpson et al. (2012), though the land cover treatment is now global in scope (Simpson et al., 2017). Importantly, the current model uses a hybrid system, which merges fine-scale data from the CORINE system over Europe (de Smet and Hettelingh, 2001), with the global GLC-2000 database (http://bioval.jrc.ec.europa.eu/products/glc2000/glc2000.php), and the more species-specific vegetation categories from the Community Land Model (CLM (Lawrence, 2011; Oleson et al., 2010). Both the GLC-2000 and CLM datasets have pros and cons. The GLC-2000 data has the advantage that nonvegetated areas such as water, ice, and urban are explicitly delineated, and also that the density of vegetation is indicated to some extent with qualifiers such as "sparse". The two main disadvantages of the GLC-2000 data for EMEP purposes are that (i) many categories consist of mixes of e.g., coniferous, and deciduous forest, and (ii) there is no distinction between ecosystem zones, e.g., no indication if a forest is boreal, temperate, or tropical. The CLM database on the other hand has clearly delineated types of forest, grouped as boreal, temperate, and tropical, and thus these are easier to handle when assigning typical foliar biomass emissions rates. In all, the EMEP model has 32 basic land-cover types, with each one assigned deposition and emission related characteristics. Fig. 3.2 shows the global forest coverage based on the EMEP land use categorization. For all figures and analyses presented herein, a lower limit of 5% forest coverage was imposed and areas below that threshold are masked.

EMEP predicts hourly values of N concentration and deposition for each grid cell and land use type within the grid cell. Given the findings of Paulot et al. (2018) and Schwede et al. (2018) of the importance of using land use specific dry deposition values over values that have been averaged across land use types in the grid cell, the results below reflect a summary using the forest-specific dry deposition from the EMP model runs. For total (wet + dry) N deposition, the forest-specific dry deposition value was combined with the grid average wet deposition value. Hourly values were summed to produce total annual fluxes as well as total fluxes for four 3-month periods with the latter being used to examine seasonal variations in deposition.

3.2 Spatial distribution of annual total deposition

Using the results from the EMEP model for 2015, the total N deposition to global forests is mapped (Fig. 3.3). In North America, the highest N deposition occurred in the eastern U.S., the central valley of California and also in southern Mexico. In South America, the highest values occurred in southern Brazil with isolated regions of high deposition in Columbia, Ecuador, and Venezuela. The countries of Germany, the Netherlands, Belgium, Italy and Switzerland had the highest values of total N deposition in Europe. In Africa, the highest deposition fluxes occurred

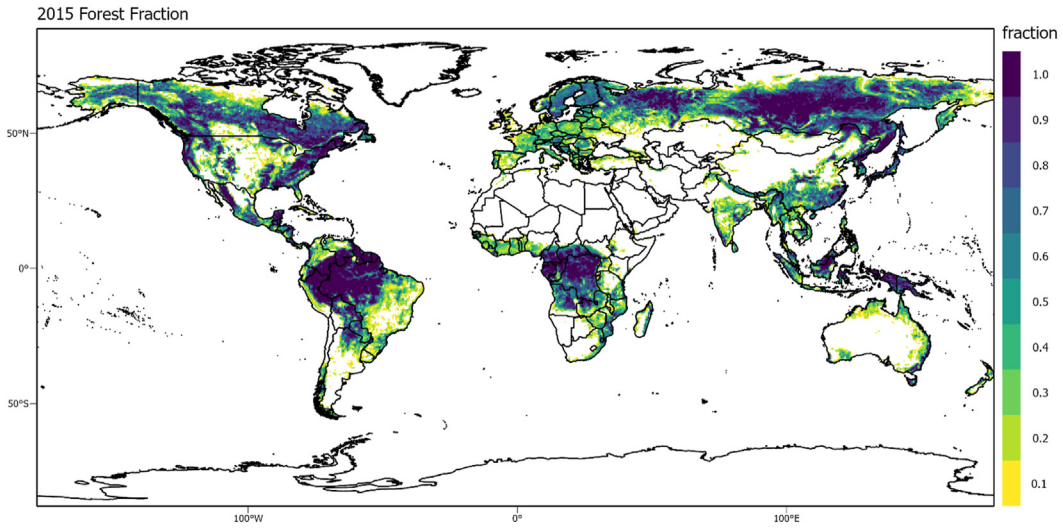

FIG. 3.2 Global forest coverage (fraction) in 0.5 × 0.5 degree grid cells as used in the EMEP modeling. Areas with less than 5% forest coverage have been masked (white color).

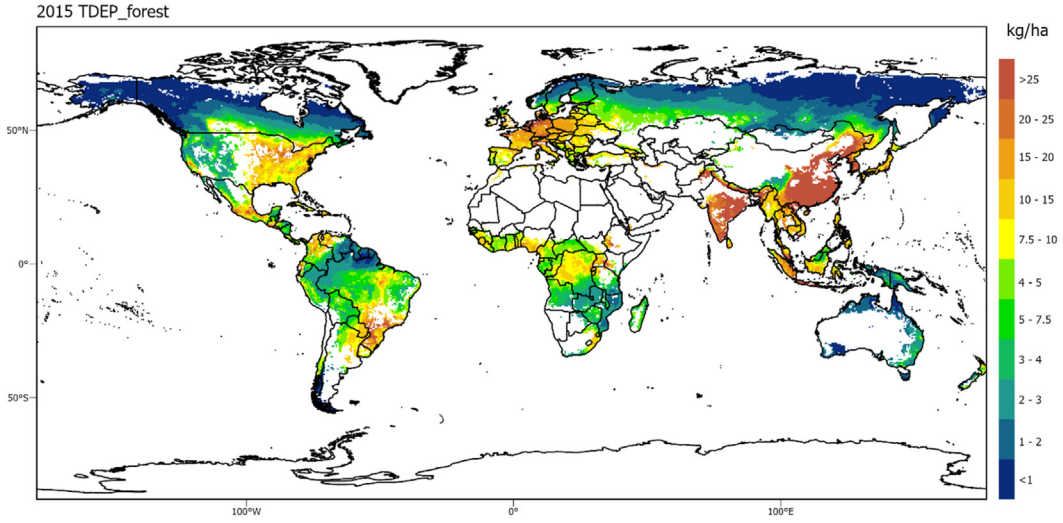

FIG. 3.3 Total (wet + dry) N deposition to forests as predicted by the EMEP model for 2015. Areas with forest cover less than 5% have been masked.

broadly in Nigeria, the Democratic Republic of the Congo (DRC), and Sierra Leone with isolated higher values in Kenya and Ethiopia. The highest N deposition over global forests occurred in broad areas of India, Nepal, China and South Korea with areas of China having deposition values in excess of 60 kg ha^{-1}.

Dividing the total deposition into reduced and oxidized N provides some indication of the sources that underlie these high values. Fig. 3.4 shows the fraction of the total N deposition that is estimated to be attributable to reduced N species. Many of the localized areas of higher deposition noted in Fig. 3.3 have at least a 50% contribution from reduced N sources and in some areas a greater than 80% contribution which likely indicates the influence of agricultural practices. However, biomass burning can also contribute to reduced N deposition as shown by Chen et al. (2010) who analyzed the N deposition to tropical forest attributable to biomass burning using the GEOS-Chem model and Bauters et al. (2018) who examined fire-derived N deposition in Africa. EMEP predicts that most nonagricultural regions are dominated by deposition of oxidized N species which can be derived from a variety of sources including energy production, motor vehicles soil NO, and biomass burning.

Fig. 3.5 provides a comparison of the relative contributions of wet and dry deposition to total N deposition. Here we see that EMEP predicts dry deposition to account for at least 50% of the total deposition in many forests of the world, especially in Europe, the U.S., Zimbabwe, and Zambia. This is an important finding as there are very few

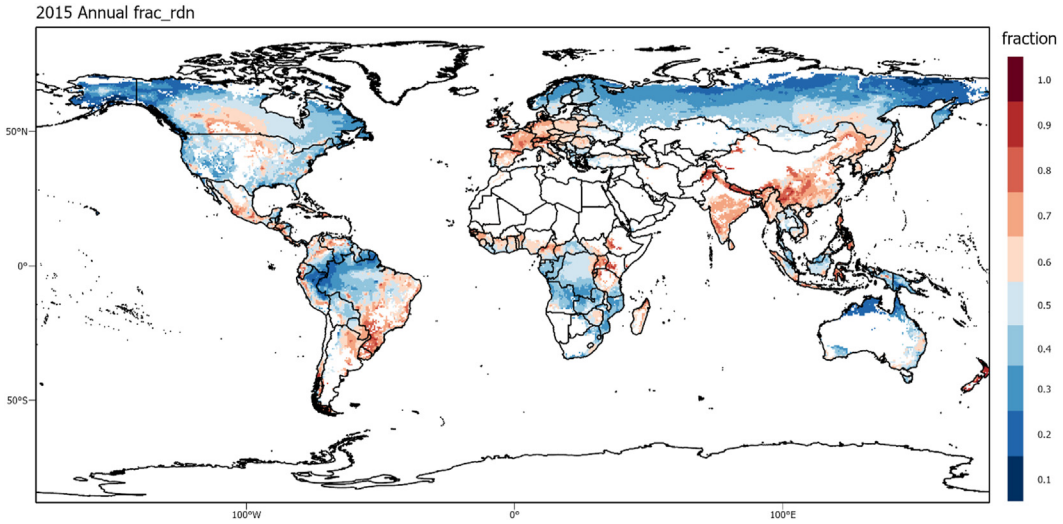

FIG. 3.4 Fraction of total N deposition that is from reduced N species as predicted by the EMEP model for 2015. Areas with forest cover less than 5% have been masked.

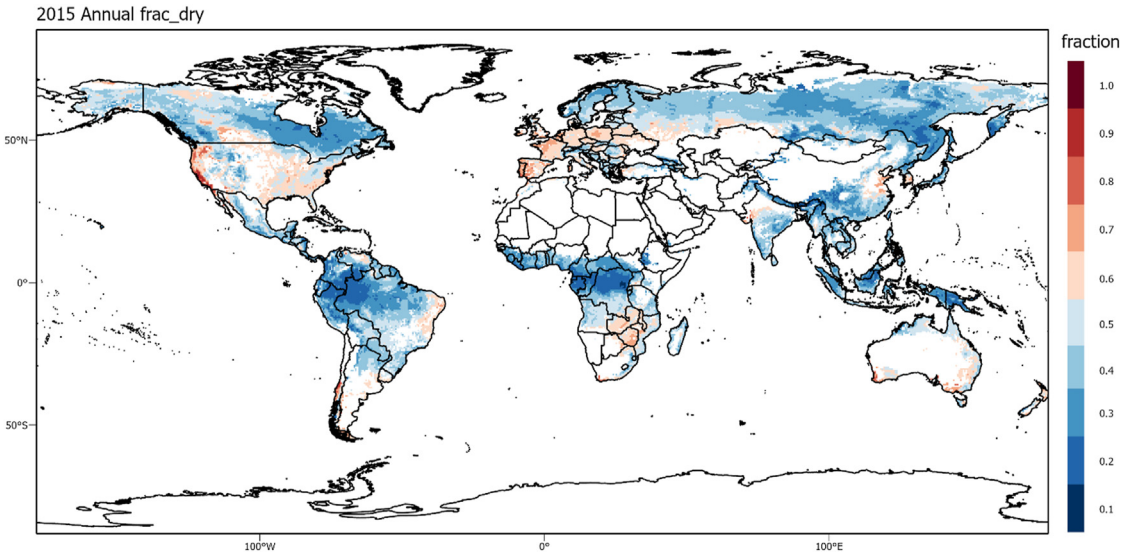

FIG. 3.5 Fraction of total N deposition that is from dry deposition as predicted by the EMEP model for 2015. Areas with forest cover less than 5% have been masked.

flux measurements of dry deposition and most are for short periods. The modeled dry deposition values are therefore an important input to the N budget emphasizing the great need for additional field studies for model development and verification to reduce uncertainties in this important component of the budget.

3.3 Spatial distribution of seasonal total deposition

Due to temporal changes in emissions, meteorology and surface parameters such as leaf area index, seasonal deposition values can be instructive in assessing impacts of N deposition to forests and informing control strategies to mitigate excess N deposition. For this analysis, we used the same four 3-month periods identified for Fig. 3.1: December, January, February (DJF; December 2015 was combined with January and February 2015); March, April, May (MAM); June, July, August (JJA), and September, October, November (SON) and calculated the total flux for each period by summing the hourly values. Seasonal values are presented as a fraction of the total annual deposition for the component plotted (e.g., wet deposition, oxidized N deposition). First, we examine seasonal variations in wet N deposition as shown in Fig. 3.6. Seasonality in wet deposition is strongly influenced by precipitation patterns such

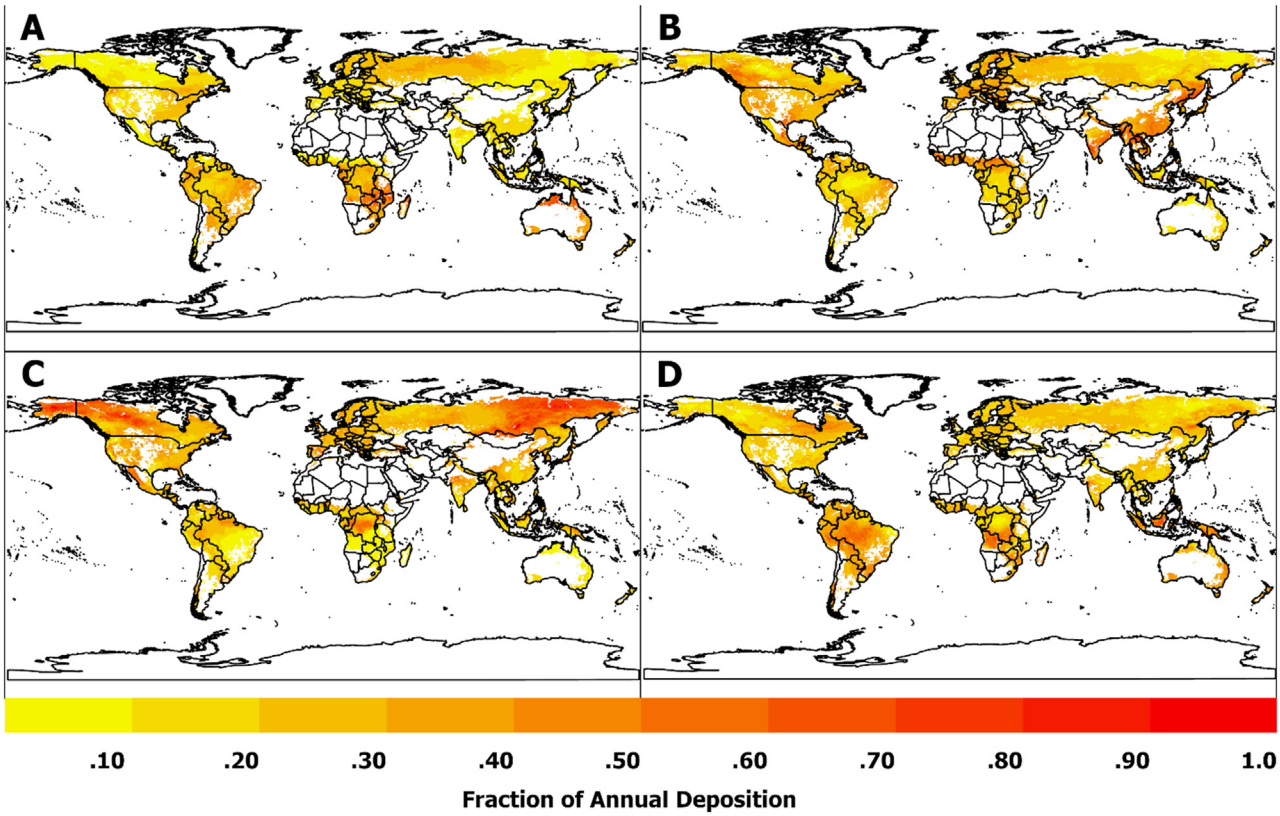

FIG. 3.6 Total seasonal wet N deposition flux predicted by the EMEP model for 3-month periods 2015 as a fraction of total wet N deposition. Areas with less than 5% forest cover have been masked. (A) is the fractional deposition for December, January, and February. (B) is the fractional deposition for March, April and May. (C) is the fractional deposition for June, July and August. (D) is the fractional deposition for September, October and November.

as those associated with monsoons in tropical areas. A strong seasonal signal in wet N deposition can be seen for south central Africa with interesting finer scale spatial variations. For example, a large fraction of wet deposition occurs in the DRC in DJF with a secondary peak in JJA while the secondary peak occurs in SON for the southern portion of DRC and Angola. For India, the highest fractional values occur in MAM. In South America, higher wet N deposition amounts are predicted to occur in SON and DJF, particularly in Brazil. Wet deposition in Russia and northwestern Canada is highest in JJA while values are highest for Europe and China in MAM. In Australia, most of the wet deposition occurs in DJF.

Dry N deposition varies seasonally due to changes in emissions, particularly those associated with agricultural practices and fires, but also meteorology and land cover changes such as leaf area index play an important role in the seasonal differences in flux. In Figs. 3.7 and 3.8, we examine the seasonal variations in oxidized and reduced dry deposition to forests, respectively. For oxidized N (Fig. 3.7), we see fairly constant flux fractions in many regions of the world such as the southeastern U.S. and Europe, reflecting a steady contribution from anthropogenic sources. More pronounced seasonal variation in oxidized N deposition can be seen in south central Africa with high values in JJA which may result from contributions from soil NO or biomass burning. Parts of Russia and Canada also show a distinct high values in JJA which may partly be due to soil NO as Simpson et al. (2023) indicate a high seasonal variability for this region, and partly due to short growing seasons where vegetation is most active and hence deposition rates greatest. For reduced N (Fig. 3.8), seasonal differences in dry deposition tend to be more localized and agree with expected patterns for agricultural activities. However, there is a quite notable seasonal difference predicted for south central Africa in the DRC and in Brazil which may be due both to agricultural practices and biomass burning. Bauters et al. (2018) note a strong impact of biomass burning on reduced N deposition in dry seasons. Russia also has relatively high values in JJA compared with other seasons which is likely due to warming temperatures and agricultural practices.

Combining the wet and dry deposition to calculate total deposition (Fig. 3.9), we see that there are important spatial differences in the seasonal values that point back to the seasonal differences in wet or dry deposition. For example, total deposition in Australia contains a stronger signal from the wet deposition component whereas total deposition in

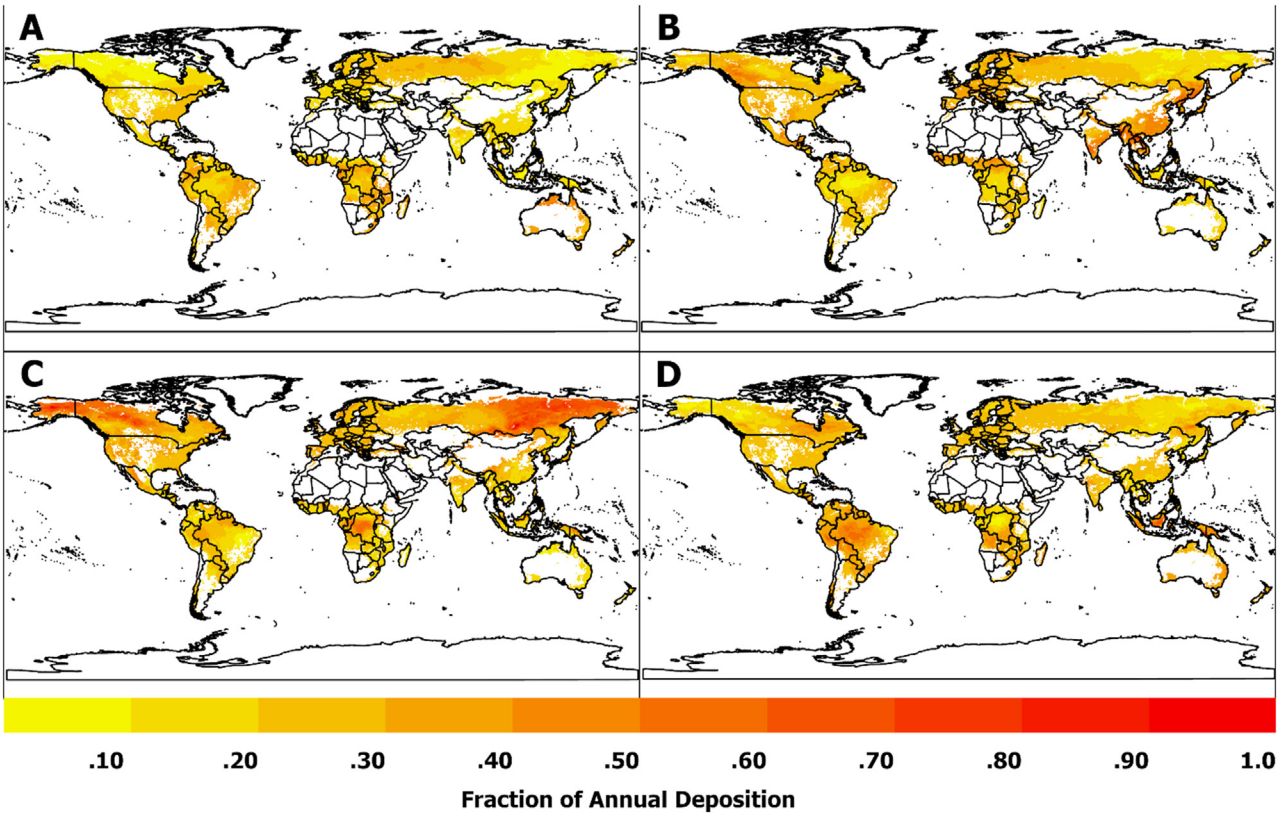

FIG. 3.7 Total seasonal dry oxidized N deposition flux predicted by EMEP for 3-month periods in 2015 as a fraction of total annual dry oxidized N deposition. Areas with less than 5% forest cover have been masked. (A) is the fractional deposition for December, January, and February. (B) is the fractional deposition for March, April and May. (C) is the fractional deposition for June, July and August. (D) is the fractional deposition for September, October and November.

the DRC reflects the influence of the dry deposition component. It should also be noted that increased wet deposition serves to cleanse the atmosphere which reduces dry deposition. The temporal patterns of each piece—dry, wet, oxidized, reduced N are all important as the temporal changes in emissions and meteorology lead to different opportunities for controlling the excess N deposition to the forests. This implies significant interactions between N deposition and forest canopies as well as seasonally different effects of N deposition on forest ecosystems.

3.4 Implications for assessing ecological effects of nitrogen deposition

This modeling analysis has useful implications for future studies on the ecological effects of N deposition in global forests. First, experimental treatments to simulate effects of N deposition usually exceed 100 kg N ha^{-1} $year^{-1}$ (Bebber, 2021), while N deposition is below 25 kg N ha^{-1} $year^{-1}$ in most forested areas, implying a gap between research and reality. Considering the nonlinear effects of N deposition (Xing et al., 2022), the high-level N treatments might result in biased predictions of the ecological effects caused by actual N deposition. Second, this modeling analysis shows that dry N deposition accounts for at least 50% of the total N deposition in many forests of the world, while most experiments simulate wet N deposition by applying N solutions. The effects of dry deposition have been rarely tested via experimental approaches and the assumption remains untested whether the dry and wet N deposition causes similar ecological effects. Third, there is a considerable variation in the ratio of reduced versus oxidized N deposition across global forests, while experimental studies often use a 1:1 ratio for reduced versus oxidized N (e.g., NH_4NO_3). Plant preference of one N form over another can have distinct ecological consequences (Boudsocq et al., 2012; Britto and Kronzucker, 2013), highlighting needed future efforts to differentiate the effects of reduced and oxidized N deposition. Finally, N deposition shows significant seasonal variations in most forests, raising the question on the ecological effects of N deposition in different seasons. Nitrogen inputs during nongrowing seasons might be subject to losses via denitrification, leaching and volatilization, while N deposition in growing season can be readily used by plants for growth, so the uncertainties in the seasonal variations in emissions

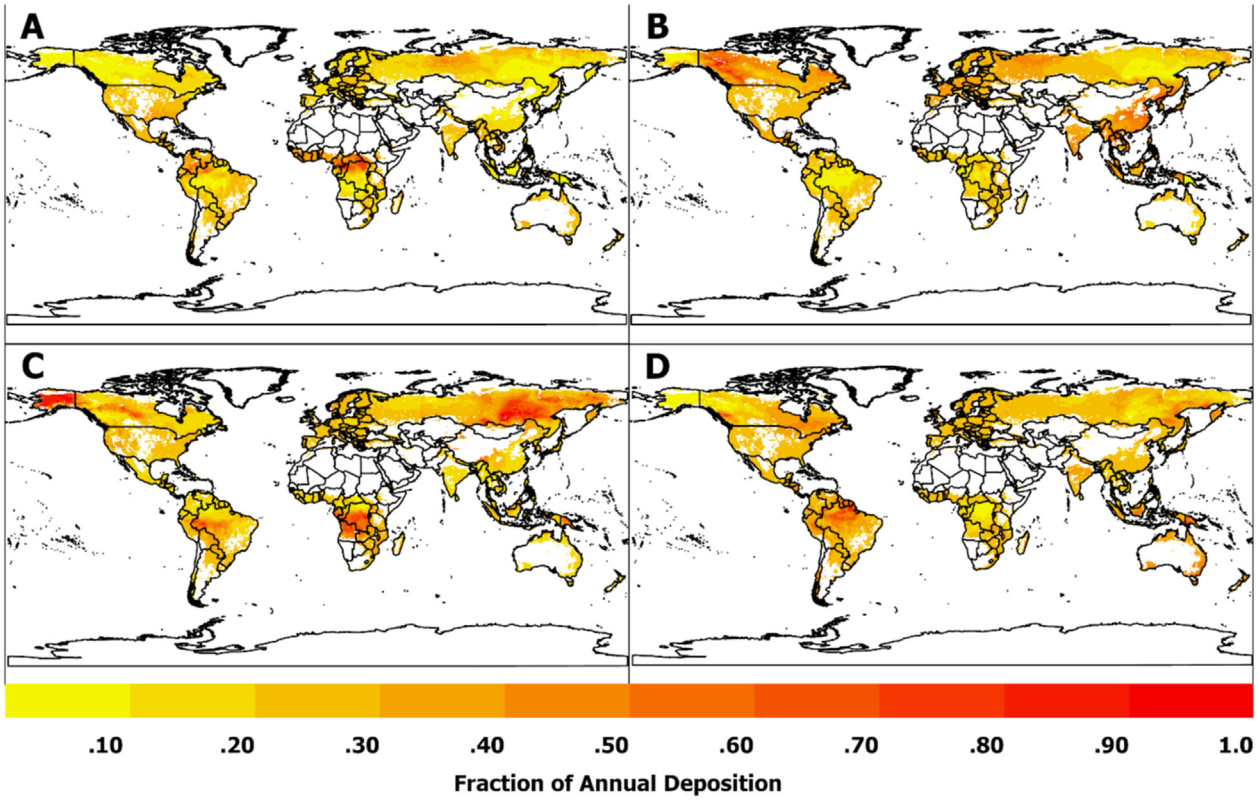

FIG. 3.8 Total seasonal dry reduced N deposition flux predicted by EMEP for 3-month periods in 2015 as a fraction of total annual dry reduced N deposition. Areas with less than 5% forest cover have been masked. (A) is the fractional deposition for December, January, and February. (B is the fractional deposition for March, April and May. (C) is the fractional deposition for June, July and August. (D) is the fractional deposition for September, October and November.

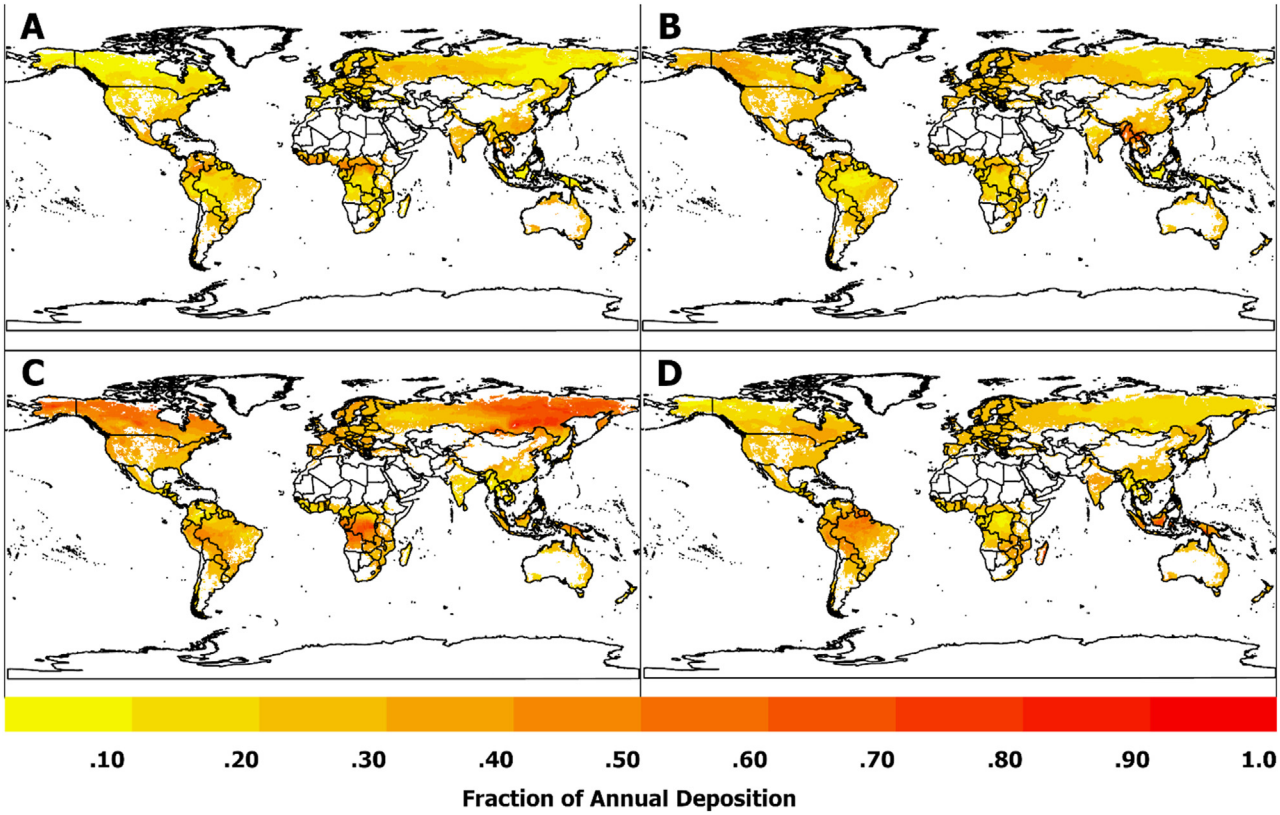

FIG. 3.9 Total seasonal deposition flux predicted by EMEP for 3-month periods in 2015 as a fraction of total annual N deposition. Areas with less than 5% forest cover have been masked. (A) is the fractional deposition for December, January, and February. (B) is the fractional deposition for March, April and May. (C) is the fractional deposition for June, July and August. (D) is the fractional deposition for September, October and November.

noted in Section 2.2 may also impact even the predicted annual N-uptake rate. However, the fates and effects of N deposition in different seasons are poorly understood.

4. Conclusions and outlook

Chemical transport models provide important information on N deposition to forests, filling in spatial gaps where deposition is not monitored and providing information on deposition of additional chemical species that are not measured. Models are particularly important for estimating global deposition of dry deposition as there are few measurements made of this important component of the total N deposition budget. There are inherent uncertainties in deposition values predicted by models and important considerations have been discussed in this chapter. Over the globe, total deposition rates of NOy and NHx species are comparable, at 56.4 and 53.6 Tg N yr^{-1}, respectively, with dry deposition accounting for ca. 28%–29% of both NOy and NHx deposition.

Spatial patterns of annual and seasonal deposition for 2015 predicted by the well-used EMEP chemical transport model were analyzed. Results demonstrate the globally varying spatial patterns of N deposition to forests. Broadly, away from populated areas, oxidized N contributes more to the total deposition than reduced N based on this study. However, deposition of reduced N can be more important in populated areas with agricultural activities. Model fluxes are sensitive to the emissions inventory used and further studies should examine this aspect. Dry deposition can contribute more than half of the total deposition in some forested areas. This demonstrates the continuing need for additional measurement studies to facilitate model development and evaluation and reduce uncertainties for this component of the total N deposition budget. Seasonal values exhibit strong spatial variability which may be associated with differences in ecological consequences. However, the analysis was limited to 1 year, implying the need for a more comprehensive analysis using a multi-year dataset to confirm the results noted here.

Acknowledgments

The views expressed in this article are those of the authors and do not necessarily represent the views or policies of the U.S. Environmental Protection Agency. We acknowledge Mark Murphy with the US EPA National Geospatial Support Team and a contractor with general Dynamics Information Technology for producing the figures of the EMEP results. Chris Clark, Kristen Foley, and John Walker of the U.S. Environmental Protection Agency provided helpful review comments and assistance with data analysis. Computer time for EMEP model runs was supported by the Research Council of Norway through the NOTUR project EMEP (NN2890K) for CPU and the NorStore project European Monitoring and Evaluation Program (NS9005K) for storage of data.

References

Ackerman, D., Millet, D.B., Chen, X., 2019. Global estimates of inorganic nitrogen deposition across four decades. Global Biogeochem. Cycles 33 (1), 100–107.

Alonso, R., Elvira, S., Sanz, M.J., Gerosa, G., Emberson, L.D., Bermejo, V., Gimeno, B.S., 2008. Sensitivity analysis of a parameterization of the stomatal component of the DO3SE model for Quercus ilex to estimate ozone fluxes. Environ. Pollut. 155 (3), 473–480.

Andersson, C., Alpfjord Wylde, H., Engardt, M., 2018. Long-term Sulfur and Nitrogen Deposition in Sweden : 1983-2013 Reanalysis. 02837730 (ISSN).

Bash, J.O., Cooter, E.J., Dennis, R.L., Walker, J.T., Pleim, J.E., 2013. Evaluation of a regional air-quality model with bidirectional NH_3 exchange coupled to an agroecosystem model. Biogeosciences 10 (3), 1635–1645.

Bauters, M., Drake, T.W., Verbeeck, H., Bodé, S., Hervé-Fernández, P., Zito, P., Podgorski, D.C., Boyemba, F., Makelele, I., Cizungu Ntaboba, L., Spencer, R.G.M., Boeckx, P., 2018. High fire-derived nitrogen deposition on central African forests. Proc. Natl. Acad. Sci. USA 115 (3), 549–554.

Beachley, G.M., Fenn, M.E., Du, E., Vries, W.d., Bauters, M., Bell, M.D., Kulshrestha, U., Schmitz, A., Walker, J.T., 2023. Monitoring nitrogen deposition in global forests: an overview of regional monitoring techniques and results. In: Du, E., Vries, W.d. (Eds.), Atmospheric Nitrogen Deposition in Global Forests: Spatial Variation, Impacts and Management Implications. Academic Press.

Bebber, D.P., 2021. The gap between atmospheric nitrogen deposition experiments and reality. Sci. Total Environ. 801, 149774.

Bergström, R., Jenkin, M.E., Hayman, G.D., Simpson, D., 2022. Update and Comparison of Atmospheric Chemistry Mechanisms for the EMEP MSC-W Model System–EmChem19a, EmChem19X, CRIv2R5Em, CB6r2Em, and MCMv3.3Em. EMEP Technical Report 1/2022. The Norwegian Meteorological Institute, Oslo, Norway. https://emep.int/publ/reports/2022/MSCW_technical_1_2022.pdf. (Accessed 15 August 2023).

Bobbink, R., Hicks, K., Galloway, J., Spranger, T., Alkemade, R., Ashmore, M., Bustamante, M., Cinderby, S., Davidson, E., Dentener, F., Emmett, B., Erisman, J.W., Fenn, M., Gilliam, F., Nordin, A., Pardo, L., De Vries, W., 2010. Global assessment of nitrogen deposition effects on terrestrial plant diversity: a synthesis. Ecol. Appl. 20 (1), 30–59.

Bocquet, M., Elbern, H., Eskes, H., Hirtl, M., Žabkar, R., Carmichael, G.R., Flemming, J., Inness, A., Pagowski, M., Pérez Camaño, J.L., Saide, P.E., San Jose, R., Sofiev, M., Vira, J., Baklanov, A., Carnevale, C., Grell, G., Seigneur, C., 2015. Data assimilation in atmospheric chemistry models: current status and future prospects for coupled chemistry meteorology models. Atmos. Chem. Phys. 15 (10), 5325–5358.

Boudsocq, S., Niboyet, A., Lata, J.C., Raynaud, X., Loeuille, N., Mathieu, J., Blouin, M., Abbadie, L., Barot, S., 2012. Plant preference for ammonium versus nitrate: a neglected determinant of ecosystem functioning? Am. Nat. 180 (1), 60–69.

Bowman, W.D., Cleveland, C.C., Halada, Ľ., Hreško, J., Baron, J.S., 2008. Negative impact of nitrogen deposition on soil buffering capacity. Nat. Geosci. 1 (11), 767–770.

Britto, D.T., Kronzucker, H.J., 2013. Ecological significance and complexity of N-source preference in plants. Ann. Bot. 112 (6), 957–963.

Bytnerowicz, A., Johnson, R.F., Zhang, L., Jenerette, G.D., Fenn, M.E., Schilling, S.L., Gonzalez-Fernandez, I., 2015. An empirical inferential method of estimating nitrogen deposition to mediterranean-type ecosystems: the San Bernardino Mountains case study. Environ. Pollut. 203, 69−88.

Chen, Y., Randerson, J.T., Van Der Werf, G.R., Morton, D.C., Mu, M., Kasibhatla, P.S., 2010. Nitrogen deposition in tropical forests from savanna and deforestation fires. Global Change Biol. 16 (7), 2024−2038.

Chiwa, M., 2021. Long-term changes in atmospheric nitrogen deposition and stream water nitrate leaching from forested watersheds in western Japan. Environ. Pollut. 287, 117634.

Cooter, E.J., Bash, J.O., Walker, J.T., Jones, M.R., Robarge, W., 2010. Estimation of NH(3) bi-directional flux from managed agricultural soils. Atmos. Environ. 44 (17), 2107−2115.

de Smet, P., Hettelingh, J.-P., 2001. Intercomparison of current land use/land cover databases. In: Posch, M., de Smet, P., Hettelingh, J.-P., Downing, R. (Eds.), Modelling and Mapping of Critical Thresholds in Europe. Status Report 2001. Coordination Centre for Effects, RIVM, Bilthoven, The Netherlands, 2001.

Deng, L., Huang, C., Kim, D.-G., Shangguan, Z., Wang, K., Song, X., Peng, C., 2020. Soil GHG fluxes are altered by N deposition: new data indicate lower N stimulation of the N_2O flux and greater stimulation of the calculated C pools. Global Change Biol. 26 (4), 2613−2629.

Dentener, F., Drevet, J., Lamarque, J.F., Bey, I., Eickhout, B., Fiore, A.M., Hauglustaine, D., Horowitz, L.W., Krol, M., Kulshrestha, U.C., Lawrence, M., Galy-Lacaux, C., Rast, S., Shindell, D., Stevenson, D., Van Noije, T., Atherton, C., Bell, N., Bergman, D., Butler, T., Cofala, J., Collins, B., Doherty, R., Ellingsen, K., Galloway, J., Gauss, M., Montanaro, V., Müller, J.F., Pitari, G., Rodriguez, J., Sanderson, M., Solmon, F., Strahan, S., Schultz, M., Sudo, K., Szopa, S., Wild, O., 2006. Nitrogen and sulfur deposition on regional and global scales: a multimodel evaluation. Global Biogeochem. Cycles 20 (4), GB4003.

Du, E., Liu, X., 2014. High rates of wet nitrogen deposition in China: a synthesis. In: Sutton, M.A., et al. (Eds.), Nitrogen Deposition, Critical Loads and Biodiversity. Springer, Dordrecht, pp. 49−56.

Du, E., Jiang, Y., Fang, J., de Vries, W., 2014. Inorganic nitrogen deposition in China's forests: status and characteristics. Atmos. Environ. 98, 474−482.

Du, E., de Vries, W., Han, W., Liu, X., Yan, Z., Jiang, Y., 2016. Imbalanced phosphorus and nitrogen deposition in China's forests. Atmos. Chem. Phys. 16 (13), 8571−8579.

Du, E., Fenn, M.E., De Vries, W., Ok, Y.S., 2019. Atmospheric nitrogen deposition to global forests: status, impacts and management options. Environ. Pollut. 250, 1044−1048.

Du, E., Terrer, C., Pellegrini, A.F., Ahlström, A., van Lissa, C.J., Zhao, X., Xia, N., Wu, X., Jackson, R.B, 2020. Global patterns of terrestrial nitrogen and phosphorus limitation. Nat. Geosci. 13 (3), 221−226.

Emberson, L.D., Ashmore, M.R., Cambridge, H.M., Simpson, D., Tuovinen, J.P., 2000. Modelling stomatal ozone flux across Europe. Environ. Pollut. 109 (3), 403−413.

Emerson, E.W., Hodshire, A.L., DeBolt, H.M., Bilsback, K.R., Pierce, J.R., McMeeking, G.R., Farmer, D.K., 2020. Revisiting particle dry deposition and its role in radiative effect estimates. Proc. Natl. Acad. Sci. USA 117 (42), 26076−26082.

Fahey, K.M., Carlton, A.G., Pye, H.O.T., Baek, J., Hutzell, W.T., Stanier, C.O., Baker, K.R., Appel, K.W., Jaoui, M., Offenberg, J.H., 2017. A framework for expanding aqueous chemistry in the Community Multiscale Air Quality (CMAQ) model version 5.1. Geosci. Model Dev 10 (4), 1587−1605.

Fenner, M., 1998. The phenology of growth and reproduction in plants. Perspect. Plant Ecol. Evol. Systemat. 1 (1), 78−91.

Flechard, C.R., Nemitz, E., Smith, R.I., Fowler, D., Vermeulen, A.T., Bleeker, A., Erisman, J.W., Simpson, D., Zhang, L., Tang, Y.S., Sutton, M.A., 2011. Dry deposition of reactive nitrogen to European ecosystems: a comparison of inferential models across the NitroEurope network. Atmos. Chem. Phys. 11 (6), 2703−2728.

Flechard, C.R., Massad, R.S., Loubet, B., Personne, E., Simpson, D., Bash, J.O., Cooter, E.J., Nemitz, E., Sutton, M.A., 2013. Advances in understanding, models and parameterizations of biosphere-atmosphere ammonia exchange. Biogeosciences 10 (7), 5183−5225.

Fowler, D., Pilegaard, K., Sutton, M.A., Ambus, P., Raivonen, M., Duyzer, J., Simpson, D., Fagerli, H., Fuzzi, S., Schjoerring, J.K., Granier, C., Neftel, A., Isaksen, I.S.A., Laj, P., Maione, M., Monks, P.S., Burkhardt, J., Daemmgen, U., Neirynck, J., Personne, E., Wichink-Kruit, R., Butterbach-Bahl, K., Flechard, C., Tuovinen, J.P., Coyle, M., Gerosa, G., Loubet, B., Altimir, N., Gruenhage, L., Ammann, C., Cieslik, S., Paoletti, E., Mikkelsen, T.N., Ro-Poulsen, H., Cellier, P., Cape, J.N., Horváth, L., Loreto, F., Niinemets, Ü., Palmer, P.I., Rinne, J., Misztal, P., Nemitz, E., Nilsson, D., Pryor, S., Gallagher, M.W., Vesala, T., Skiba, U., Brüggemann, N., Zechmeister-Boltenstern, S., Williams, J., O'Dowd, C., Facchini, M.C., de Leeuw, G., Flossman, A., Chaumerliac, N., Erisman, J.W., 2009. Atmospheric composition change: ecosystems−atmosphere interactions. Atmos. Environ. 43 (33), 5193−5267.

Fu, Y., Wang, W., Han, M., Kuerban, M., Wang, C., Liu, X., 2019. Atmospheric dry and bulk nitrogen deposition to forest environment in the North China Plain. Atmos. Pollut. Res. 10 (5), 1636−1642.

Fu, J.S., Carmichael, G.R., Dentener, F., Aas, W., Andersson, C., Barrie, L.A., Cole, A., Galy-Lacaux, C., Geddes, J., Itahashi, S., Kanakidou, M., Labrador, L., Paulot, F., Schwede, D., Tan, J., Vet, R., 2022. Improving estimates of sulfur, nitrogen, and ozone total deposition through multi-model and measurement-model fusion approaches. Environ. Sci. Technol. 56 (4), 2134−2142.

Galmarini, S., Makar, P., Clifton, O., Hogrefe, C., Bash, J., Bianconi, R., Bellasio, R., Bieser, J., Butler, T., Ducker, J., Flemming, J., Hozdic, A., Holmes, C., Kioutsioukis, I., Kranenburg, R., Lupascu, A., Perez-Camanyo, J.L., Pleim, J., Ryu, Y.H., San Jose, R., Schwede, D., Silva, S., Garcia Vivanco, M., Wolke, R., 2021. Technical note−AQMEII4 activity 1: evaluation of wet and dry deposition schemes as an integral part of regional-scale air quality models. Atmos. Chem. Phys. Discuss. 2021, 1−53.

García-Gómez, H., Izquieta-Rojano, S., Aguillaume, L., González-Fernández, I., Valiño, F., Elustondo, D., Santamaría, J.M., Àvila, A., Bytnerowicz, A., Bermejo, V., Alonso, R., 2018. Joining empirical and modelling approaches to estimate dry deposition of nitrogen in Mediterranean forests. Environ. Pollut. 243, 427−436.

Gilliam, F.S., Burns, D.A., Driscoll, C.T., Frey, S.D., Lovett, G.M., Watmough, S.A., 2019. Decreased atmospheric nitrogen deposition in eastern North America: predicted responses of forest ecosystems. Environ. Pollut. 244, 560−574.

Granier, C., Darras, S., Denier Van Der Gon, H., Jana, d., Elguindi, N., Bo, g., Michael, g., Marc, g., Jalkanen, J.-P., Kuenen, J., Liousse, C., Quack, B., Simpson, D., Sindelarova, K., 2019. The Copernicus

Atmosphere Monitoring Service Global and Regional Emissions (April 2019 Version). Copernicus Atmosphere Monitoring Service.

Guevara, M., Jorba, O., Tena, C., Denier van der Gon, H., Kuenen, J., Elguindi, N., Darras, S., Granier, C., Pérez García-Pando, C., 2021. Copernicus Atmosphere Monitoring Service TEMPOral profiles (CAMS-TEMPO): global and European emission temporal profile maps for atmospheric chemistry modelling. Earth Syst. Sci. Data 13 (2), 367−404.

Gurmesa, G.A., Wang, A., Li, S., Peng, S., de Vries, W., Gundersen, P., Ciais, P., Phillips, O.L., Hobbie, E.A., Zhu, W., Nadelhoffer, K., Xi, Y., Bai, E., Sun, T., Chen, D., Zhou, W., Zhang, Y., Guo, Y., Zhu, J., Duan, L., Li, D., Koba, K., Du, E., Zhou, G., Han, X., Han, S., Fang, Y., 2022. Retention of deposited ammonium and nitrate and its impact on the global forest carbon sink. Nat. Commun. 13 (1), 880.

Hansen, K., Sørensen, L.L., Hertel, O., Geels, C., Skjøth, C.A., Jensen, B., Boegh, E., 2013. Ammonia emissions from deciduous forest after leaf fall. Biogeosciences 10 (7), 4577−4589.

Ignatova, N., Dambrine, É., 2000. Canopy uptake of N deposition in spruce (*Picea abies* L. Karst) stands. Ann. For. Sci. 57 (2), 113−120.

International Institute for Applied Systems Analysis, 2021. ECLIPSE V6b Global Emission Fields.

Itahashi, S., Ge, B., Sato, K., Fu, J.S., Wang, X., Yamaji, K., Nagashima, T., Li, J., Kajino, M., Liao, H., Zhang, M., Wang, Z., Li, M., Kurokawa, J., Carmichael, G.R., Wang, Z., 2020. MICS-Asia III: overview of model intercomparison and evaluation of acid deposition over Asia. Atmos. Chem. Phys. 20 (5), 2667−2693.

Jonson, J.E., Schulz, M., Emmons, L., Flemming, J., Henze, D., Sudo, K., Tronstad Lund, M., Lin, M., Benedictow, A., Koffi, B., Dentener, F., Keating, T., Kivi, R., Davila, Y., 2018. The effects of intercontinental emission sources on European air pollution levels. Atmos. Chem. Phys. 18 (18), 13655−13672.

Kanakidou, M., Myriokefalitakis, S., Daskalakis, N., Fanourgakis, G., Nenes, A., Baker, A.R., Tsigaridis, K., Mihalopoulos, N., 2016. Past, present, and future atmospheric nitrogen deposition. J. Atmos. Sci. 73 (5), 2039−2047.

Katata, G., 2014. Fogwater deposition modeling for terrestrial ecosystems: a review of developments and measurements. J. Geophys. Res. Atmos. 119 (13), 8137−8159.

Keenan, R.J., Reams, G.A., Achard, F., de Freitas, J.V., Grainger, A., Lindquist, E., 2015. Dynamics of global forest area: results from the FAO global forest resources assessment 2015. For. Ecol. Manag. 352, 9−20.

Klimont, Z., Kupiainen, K., Heyes, C., Purohit, P., Cofala, J., Rafaj, P., Borken-Kleefeld, J., Schöpp, W., 2017. Global anthropogenic emissions of particulate matter including black carbon. Atmos. Chem. Phys. 17 (14), 8681−8723.

Kouznetsov, R., Sofiev, M., 2012. A methodology for evaluation of vertical dispersion and dry deposition of atmospheric aerosols. J. Geophys. Res. Atmos. 117 (D1).

Kulshrestha, U.C., Kulshrestha, M.J., Satyanarayana, J., Reddy, L.A.K., 2014. Atmospheric deposition of reactive nitrogen in India. In: Sutton, M.A., et al. (Eds.), Nitrogen Deposition, Critical Loads and Biodiversity. Springer Netherlands, Dordrecht, pp. 75−82.

Lamarque, J.F., Dentener, F., McConnell, J., Ro, C.U., Shaw, M., Vet, R., Bergmann, D., Cameron-Smith, P., Dalsoren, S., Doherty, R., Faluvegi, G., Ghan, S.J., Josse, B., Lee, Y.H., MacKenzie, I.A., Plummer, D., Shindell, D.T., Skeie, R.B., Stevenson, D.S., Strode, S., Zeng, G., Curran, M., Dahl-Jensen, D., Das, S., Fritzsche, D., Nolan, M., 2013. Multi-model mean nitrogen and sulfur deposition from the Atmospheric Chemistry and Climate Model Intercomparison Project (ACCMIP): evaluation of historical and projected future changes. Atmos. Chem. Phys. 13 (16), 7997−8018.

Lawrence, D.M., 2011. Parameterization improvements and functional and structural advances in version 4 of the community land model. J. Adv. Model. Earth Syst. 3, M03001.

Li, Y., Schichtel, B.A., Walker, J.T., Schwede, D.B., Chen, X., Lehmann, C.M.B., Puchalski, M.A., Gay, D.A., Collett, J.L., 2016. Increasing importance of deposition of reduced nitrogen in the United States. Proc. Natl. Acad. Sci. USA 113 (21), 5874−5879.

Liu, X., Zhang, Y., Han, W., Tang, A., Shen, J., Cui, Z., Vitousek, P., Erisman, J.W., Goulding, K., Christie, P., Fangmeier, A., Zhang, F., 2013. Enhanced nitrogen deposition over China. Nature 494 (7438), 459−462.

Liu, L., Zhang, X., Lu, X., 2016. The composition, seasonal variation, and potential sources of the atmospheric wet sulfur (S) and nitrogen (N) deposition in the southwest of China. Environ. Sci. Pollut. Control Ser. 23 (7), 6363−6375.

Lovett, G.M., Lindberg, S.E., 1993. Atmospheric deposition and canopy interactions of nitrogen in forests. Can. J. For. Res. 23 (8), 1603−1616.

Marchetto, A., Simpson, D., Aas, W., Fagerli, H., Hansen, K., Pihl-Karlsson, G., Karlsson, P.E., Rogora, M., Sanders, T.G.M., Schmitz, A., Seidling, W., Thimonier, A., Tsyro, S., de Vries, W., Waldner, P., 2021. Good agreement between modeled and measured sulfur and nitrogen deposition in Europe, in spite of marked differences in some sites. Front. Environ. Sci. 9 (400).

Massad, R.S., Nemitz, E., Sutton, M.A., 2010. Review and parameterisation of bi-directional ammonia exchange between vegetation and the atmosphere. Atmos. Chem. Phys. 10 (21), 10359−10386.

Neff, J.C., Holland, E.A., Dentener, F., McDowell, W.H., Russell, K.M., 2002. The origin, composition and rates of organic nitrogen deposition: a missing piece of the nitrogen cycle? Biogeochemistry 57−58 (1), 99−136.

Nemitz, E., Milford, C., Sutton, M.A., 2001. A two-layer canopy compensation point model for describing bi-directional biosphere-atmosphere exchange of ammonia. Q. J. R. Meteorol. Soc. 127 (573), 815−833.

Oleson, K., Lawrence, D., Bonan, G., Flanner, M., Kluzek, E., Lawrence, P., Levis, S., Swenson, S., Thornton, P., Dai, A., Decker, M., Dickinson, R., Feddema, J., Heald, C., Hoffman, F., Lamarque, J.F., Mahowald, N., Niu, G.Y., Qian, T., Randerson, J., Running, S., Sakaguchi, K., Slater, A., Stockli, R., Wang, A., Yang, Z.L., Zeng, X., Zeng, X., 2010. Technical Description of Version 4.0 of the Community Land Model (CLM) (No. NCAR/TN-478+STR). University Corporation for Atmospheric Research.

Paulot, F., Malyshev, S., Nguyen, T., Crounse, J.D., Shevliakova, E., Horowitz, L.W., 2018. Representing sub-grid scale variations in nitrogen deposition associated with land use in a global Earth system model: implications for present and future nitrogen deposition fluxes over North America. Atmos. Chem. Phys. 18 (24), 17963−17978.

Peñuelas, J., Poulter, B., Sardans, J., Ciais, P., van der Velde, M., Bopp, L., Boucher, O., Godderis, Y., Hinsinger, P., Llusia, J., Nardin, E., Vicca, S., Obersteiner, M., Janssens, I.A., 2013. Human-induced nitrogen−phosphorus imbalances alter natural and managed ecosystems across the globe. Nat. Commun. 4 (1), 2934.

Petroff, A., Zhang, L., 2010. Development and validation of a size-resolved particle dry deposition scheme for application in aerosol transport models. Geosci. Model Dev. 3 (2), 753−769.

Petroff, A., Mailliat, A., Amielh, M., Anselmet, F., 2008a. Aerosol dry deposition on vegetative canopies. Part I: review of present knowledge. Atmos. Environ. 42 (16), 3625−3653.

Petroff, A., Mailliat, A., Amielh, M., Anselmet, F., 2008b. Aerosol dry deposition on vegetative canopies. Part II: a new modelling approach and applications. Atmos. Environ. 42 (16), 3654−3683.

Piao, S., Liu, Q., Chen, A., Janssens, I.A., Fu, Y., Dai, J., Liu, L., Lian, X., Shen, M., Zhu, X., 2019. Plant phenology and global climate change: current progresses and challenges. Global Change Biol. 25 (6), 1922−1940.

Pleim, J.E., Bash, J.O., Walker, J.T., Cooter, E.J., 2013. Development and evaluation of an ammonia bidirectional flux parameterization for air quality models. J. Geophys. Res. Atmos. 118 (9), 3794−3806.

Pryor, S.C., Barthelmie, R.J., Jensen, B., Jensen, N.O., Sorensen, L.L., 2002. HNO3 fluxes to a deciduous forest derived using gradient and REA methods. Atmos. Environ. 36 (39−40), 5993−5999.

Pryor, S.C., Gallagher, M., Sievering, H., Larsen, S.E., Barthelmie, R.J., Birsan, F., Nemitz, E., Rinne, J., Kulmala, M., Groenholm, T., Taipale, R., Vesala, T., 2008. A review of measurement and modelling results of particle atmosphere-surface exchange. Tellus Ser. B Chem. Phys. Meteorol. 60 (1), 42−75.

Raivonen, M., Vesala, T., Pirjola, L., Altimir, N., Keronen, P., Kulmala, M., Hari, P., 2009. Compensation point of NOx exchange: net result of NOx consumption and production. Agric. For. Meteorol. 149, 1073−1081.

Sander, R., 2015. Compilation of Henry's law constants (version 4.0) for water as solvent. Atmos. Chem. Phys. 15 (8), 4399−4981.

Sandu, A., Chai, T., 2011. Chemical data assimilation—an overview. Atmosphere 2 (3), 426−463.

Saylor, R.D., Baker, B.D., Lee, P., Tong, D., Pan, L., Hicks, B.B., 2019. The particle dry deposition component of total deposition from air quality models: right, wrong or uncertain? Tellus B 71 (1), 1550324.

Schmitz, A., Sanders, T.G.M., Bolte, A., Bussotti, F., Dirnböck, T., Johnson, J., Peñuelas, J., Pollastrini, M., Prescher, A.-K., Sardans, J., Verstraeten, A., de Vries, W., 2019. Responses of forest ecosystems in Europe to decreasing nitrogen deposition. Environ. Pollut. 244, 980−994.

Schulte-Uebbing, L., de Vries, W., 2018. Global-scale impacts of nitrogen deposition on tree carbon sequestration in tropical, temperate, and boreal forests: a meta-analysis. Global Change Biol. 24 (2), e416−e431.

Schulte-Uebbing, L.F., Ros, G.H., de Vries, W., 2022. Experimental evidence shows minor contribution of nitrogen deposition to global forest carbon sequestration. Global Change Biol. 28 (3), 899−917.

Schwede, D.B., Lear, G.G., 2014. A novel hybrid approach for estimating total deposition in the United States. Atmos. Environ. 92 (0), 207−220.

Schwede, D., Zhang, L., Vet, R., Lear, G., 2011. An intercomparison of the deposition models used in the CASTNET and CAPMoN networks. Atmos. Environ. 45 (6), 1337−1346.

Schwede, D.B., Simpson, D., Tan, J., Fu, J.S., Dentener, F., Du, E., deVries, W., 2018. Spatial variation of modelled total, dry and wet nitrogen deposition to forests at global scale. Environ. Pollut. 243, 1287−1301.

Schwede, D., Cole, A., Vet, R., Lear, G., 2019. Ongoing U.S.-Canada Collaboration on Nitrogen and Sulfur Deposition. EM Magazine, June.

Simkin, S.M., Allen, E.B., Bowman, W.D., Clark, C.M., Belnap, J., Brooks, M.L., Cade, B.S., Collins, S.L., Geiser, L.H., Gilliam, F.S., Jovan, S.E., Pardo, L.H., Schulz, B.K., Stevens, C.J., Suding, K.N., Throop, H.L., Waller, D.M., 2016. Conditional vulnerability of plant diversity to atmospheric nitrogen deposition across the United States. Proc. Natl. Acad. Sci. USA 113 (15), 4086−4091.

Simpson, D., Butterbach-Bahl, K., Fagerli, H., Kesik, M., Skiba, U., Tang, S., 2006. Deposition and emissions of reactive nitrogen over European forests: a modelling study. Atmos. Environ. 40 (29), 5712−5726.

Simpson, D., Benedictow, A., Berge, H., Bergström, R., Emberson, L.D., Fagerli, H., Flechard, C.R., Hayman, G.D., Gauss, M., Jonson, J.E., Jenkin, M.E., Nyíri, A., Richter, C., Semeena, V.S., Tsyro, S., Tuovinen, J.P., Valdebenito, Á., Wind, P., 2012. The EMEP MSC-W chemical transport model−technical description. Atmos. Chem. Phys. 12 (16), 7825−7865.

Simpson, D., Bergström, R., Imhof, H., Wind, P., 2017. Updates to the EMEP/MSC-W Model, 2016−2017. The Norwegian Meteorological Institute, Oslo, Norway.

Simpson, D., Benedictow, A.M.L., Darras, S., 2023. The CAMS soil emissions: CAMS-GLOB- SOIL. In: CAMS2_61 − Global and European emission inventories. Contribution to documentation of products provided by CAMS2_61 (Eds. Denier van der Gon, H., Gauss, M., and Granier, C), Awaiting doi. Copernicus Atmospheric Monitoring Service. In press.

Simpson, D., Bergström, R., Briolat, A., Imhof, H., Johansson, J., Priestley, M., Valdebenito, A., 2020. GenChem v1.0−a chemical pre-processing and testing system for atmospheric modelling. Geosci. Model Dev. (GMD) 13 (12), 6447−6465.

Simpson, D., Gauss, M., Mu, Q., Tsyro, S., Valdebento, A., Wind, P., 2021. Updates to the EMEP/MSC-W Model, 2020–2021, Transboundary Particulate Matter, Photo-Oxidants, Acidifying and Eutrophying Components. EMEP Status Report 1/2021. Norwegian Meteorological Institute, Oslo, Norway, pp. 109−121.

Slinn, W.G.N., 1982. Predictions for particle deposition to vegetative canopies. Atmos. Environ. 16 (7), 1785−1794.

Sparks, J.P., 2009. Ecological ramifications of the direct foliar uptake of nitrogen. Oecologia 159 (1), 1−13.

Tan, J., Fu, J.S., Dentener, F., Sun, J., Emmons, L., Tilmes, S., Sudo, K., Flemming, J., Jonson, J.E., Gravel, S., Bian, H., Davila, Y., Henze, D.K., Lund, M.T., Kucsera, T., Takemura, T., Keating, T., 2018. Multi-model study of HTAP II on sulfur and nitrogen deposition. Atmos. Chem. Phys. 18 (9), 6847−6866.

Tang, Y.S., Flechard, C.R., Dämmgen, U., Vidic, S., Djuricic, V., Mitosinkova, M., Uggerud, H.T., Sanz, M.J., Simmons, I., Dragosits, U., Nemitz, E., Twigg, M., van Dijk, N., Fauvel, Y., Sanz, F., Ferm, M., Perrino, C., Catrambone, M., Leaver, D., Braban, C.F., Cape, J.N., Heal, M.R., Sutton, M.A., 2021. Pan-European rural monitoring network shows dominance of NH_3 gas and NH_4NO_3 aerosol in inorganic atmospheric pollution load. Atmos. Chem. Phys. 21 (2), 875−914.

Theobald, M.R., Vivanco, M.G., Aas, W., Andersson, C., Ciarelli, G., Couvidat, F., Cuvelier, K., Manders, A., Mircea, M., Pay, M.T., Tsyro, S., Adani, M., Bergström, R., Bessagnet, B., Briganti, G., Cappelletti, A., D'Isidoro, M., Fagerli, H., Mar, K., Otero, N.,

Raffort, V., Roustan, Y., Schaap, M., Wind, P., Colette, A., 2019. An evaluation of European nitrogen and sulfur wet deposition and their trends estimated by six chemistry transport models for the period 1990–2010. Atmos. Chem. Phys. 19 (1), 379–405.

Vet, R., Artz, R.S., Carou, S., 2014. A global assessment of precipitation chemistry and deposition of sulfur, nitrogen, sea salt, base cations, organic acids, acidity and pH, and phosphorus. Atmos. Environ. 93, 1–2.

Vivanco, M.G., Theobald, M.R., García-Gómez, H., Garrido, J.L., Prank, M., Aas, W., Adani, M., Alyuz, U., Andersson, C., Bellasio, R., Bessagnet, B., Bianconi, R., Bieser, J., Brandt, J., Briganti, G., Cappelletti, A., Curci, G., Christensen, J.H., Colette, A., Couvidat, F., Cuvelier, C., D'Isidoro, M., Flemming, J., Fraser, A., Geels, C., Hansen, K.M., Hogrefe, C., Im, U., Jorba, O., Kitwiroon, N., Manders, A., Mircea, M., Otero, N., Pay, M.T., Pozzoli, L., Solazzo, E., Tsyro, S., Unal, A., Wind, P., Galmarini, S., 2018. Modeled deposition of nitrogen and sulfur in Europe estimated by 14 air quality model systems: evaluation, effects of changes in emissions and implications for habitat protection. Atmos. Chem. Phys. 18 (14), 10199–10218.

Waldner, P., Marchetto, A., Thimonier, A., Schmitt, M., Rogora, M., Granke, O., Mues, V., Hansen, K., Pihl Karlsson, G., Žlindra, D., Clarke, N., Verstraeten, A., Lazdins, A., Schimming, C., Iacoban, C., Lindroos, A.-J., Vanguelova, E., Benham, S., Meesenburg, H., Nicolas, M., Kowalska, A., Apuhtin, V., Napa, U., Lachmanová, Z., Kristoefel, F., Bleeker, A., Ingerslev, M., Vesterdal, L., Molina, J., Fischer, U., Seidling, W., Jonard, M., O'Dea, P., Johnson, J., Fischer, R., Lorenz, M., 2014. Detection of temporal trends in atmospheric deposition of inorganic nitrogen and sulphate to forests in Europe. Atmos. Environ. 95, 363–374.

Walker, J.T., Beachley, G., Amos, H.M., Baron, J.S., Bash, J., Baumgardner, R., Bell, M.D., Benedict, K.B., Chen, X., Clow, D.W., Cole, A., Coughlin, J.G., Cruz, K., Daly, R.W., Decina, S.M., Elliott, E.M., Fenn, M.E., Ganzeveld, L., Gebhart, K., Isil, S.S., Kerschner, B.M., Larson, R.S., Lavery, T., Lear, G.G., Macy, T., Mast, M.A., Mishoe, K., Morris, K.H., Padgett, P.E., Pouyat, R.V., Puchalski, M., Pye, H.O.T., Rea, A.W., Rhodes, M.F., Rogers, C.M., Saylor, R., Scheffe, R., Schichtel, B.A., Schwede, D.B., Sexstone, G.A., Sive, B.C., Sosa Echeverría, R., Templer, P.H., Thompson, T., Tong, D., Wetherbee, G.A., Whitlow, T.H., Wu, Z., Yu, Z., Zhang, L., 2019. Toward the improvement of total nitrogen deposition budgets in the United States. Sci. Total Environ. 691, 1328–1352.

Wang, X., Zhang, L., Moran, M.D., 2010. Uncertainty assessment of current size-resolved parameterizations for below-cloud particle scavenging by rain. Atmos. Chem. Phys. 10 (12), 5685–5705.

Wang, R., Goll, D., Balkanski, Y., Hauglustaine, D., Boucher, O., Ciais, P., Janssens, I., Penuelas, J., Guenet, B., Sardans, J., Bopp, L., Vuichard, N., Zhou, F., Li, B., Piao, S., Peng, S., Huang, Y., Tao, S., 2017. Global forest carbon uptake due to nitrogen and phosphorus deposition from 1850 to 2100. Global Change Biol. 23 (11), 4854–4872.

Wen, Z., Xu, W., Li, Q., Han, M., Tang, A., Zhang, Y., Luo, X., Shen, J., Wang, W., Li, K., Pan, Y., Zhang, L., Li, W., Collett, J.L., Zhong, B., Wang, X., Goulding, K., Zhang, F., Liu, X., 2020. Changes of nitrogen deposition in China from 1980 to 2018. Environ. Int. 144, 106022.

Wesely, M.L., Hicks, B.B., 2000. A review of the current status of knowledge on dry deposition. Atmos. Environ. 34 (12–14), 2261–2282.

Wesely, M.L., 1989. Parameterization of surface resistances to gaseous dry deposition in regional-scale numerical models. Atmos. Environ. 23 (6), 1293–1304.

Wu, Z., Schwede, D.B., Vet, R., Walker, J.T., Shaw, M., Staebler, R., Zhang, L., 2018. Evaluation and intercomparison of five North American dry deposition algorithms at a mixed forest site. J. Adv. Model. Earth Syst. 10 (7), 1571–1586.

Xia, N., Du, E.Z., Wu, X.H., Tang, Y., Wang, Y., de Vries, W., 2020. Effects of nitrogen addition on soil methane uptake in global forest biomes. Environ. Pollut. 264.

Xing, A., Du, E., Shen, H., Xu, L., de Vries, W., Zhao, M., Liu, X., Fang, J., 2022. Nonlinear responses of ecosystem carbon fluxes to nitrogen deposition in an old-growth boreal forest. Ecol. Lett. 25 (1), 77–88.

Zhang, L., He, Z., 2014. Technical note: an empirical algorithm estimating dry deposition velocity of fine, coarse and giant particles. Atmos. Chem. Phys. 14 (7), 3729–3737.

Zhang, J., Shao, Y., 2014. A new parameterization of particle dry deposition over rough surfaces. Atmos. Chem. Phys. 14 (22), 12429–12440.

Zhang, L., Brook, J.R., Vet, R., 2003. A revised parameterization for gaseous dry deposition in air-quality models. Atmos. Chem. Phys. 3 (6), 2067–2082.

Zhang, L., Wang, X., Moran, M.D., Feng, J., 2013. Review and uncertainty assessment of size-resolved scavenging coefficient formulations for below-cloud snow scavenging of atmospheric aerosols. Atmos. Chem. Phys. 13 (19), 10005–10025.

Zhang, Y., Foley, K.M., Schwede, D.B., Bash, J.O., Pinto, J.P., Dennis, R.L., 2019. A measurement-model fusion approach for improved wet deposition maps and trends. J. Geophys. Res. Atmos. 124 (7), 4237–4251.

Zhao, Y., Zhang, L., Pan, Y., Wang, Y., Paulot, F., Henze, D.K., 2015. Atmospheric nitrogen deposition to the northwestern Pacific: seasonal variation and source attribution. Atmos. Chem. Phys. 15 (18), 10905–10924.